University of Michigan Human Powered Submarine

Wolverine

For ISR 13
June 22-26, 2015

Contents

Team Introduction:

The University of Michigan Human Powered Submarine team has been around since 1997, competing in both the ISR and EISR competitions. The team is student run and currently comprised of all undergraduate students. The team is comprised of a variety of students, including mechanical, naval, nuclear, and electrical engineering, as well as material sciences and computer science. All University of Michigan students are welcome to join.

Team Organization

The University of Michigan team is a fully student run, extra-curricular team within the college of engineering. Student participation is purely volunteer, they receive no course credit and fulfil no requirements by joining the team. Instead students join to increase their engineering skills, challenge themselves, and to get a chance to work on a hands on project.

The team has a faculty advisor in the Naval Architecture and Marine Engineering department but all administrative and technical decisions are made by the team alone. The team leadership is broken up into an administrative leader, the president, and technical leader, the design manager. The technical aspects were then broken down until individual systems and assigned to different students. Those students, with the help of the design manager, were in charge of designing and testing the systems. The bulk of the rest of the team helped primarily with manufacturing. The team this year was very young, with only seven returning members from last year out of about fifteen members. Only two members have been to the ISR before. That posed a challenge for the team this year, as few people had enough experience to lead a system, but will provide an asset in years to come.

Team Finances

The university provides us with a space dedicated to project teams that includes mills, lathes, and a router. That is a huge asset because it gives us a permanent space to work and store our materials. The rest of our funding must be acquired by the team members. About half of our cash funding comes from university departments that are represented by team members. The rest of our funding comes from companies either in the form of cash or materials. Corporations sponsor us with monetary and material donations in exchange for publicity and an advantage recruiting students for employment. The team's presence at industry conferences and events was crucial in securing sponsorships. Our title sponsor this year was Caterpillar Marine, who were instrumental in helping the team compete this year. Please see the rest of our sponsors on the last page of this report.

Hull:

This year we opted to return to an older hull design that we used in the previous ISR. We built a new hull last year for the EISR but it had pronounced stability issues. We conducted wind tunnel tests to compare the two hulls, Wolverine (raced in the 2013 ISR) and Odyssey (raced in the 2014 EISR). In the wind tunnel we tested at 26.1 m/s which is equivalent to 0.46 knots through water. This is due to Reynolds number scaling, which takes into account a 15% scale model and the density change. Due to the top speed of the wind tunnel being much lower than required for Reynolds scaling, we matched the Reynolds number divided by ten. This is an acceptable approximation because we are comparing the two models to each other, not with the actual submarine. The models were yawed 10 degrees in each direction at both speeds to assess stability.

The models were made in two halves on the router and glued together and faired. The scaled down control surfaces were made on a 3D printer.

The wind tunnel tests were used to verify computational fluid dynamics (CFD) analysis of drag and determine stability, which couldn't be accurately done with CFD. Both models were shown to be stable within the 10 degree yaw we tested. The CFD and wind tunnel tests showed Odyssey had a slightly lower drag coefficient, but much higher pressure coefficient and drag area. This data is displayed in Figure 1.1. This means that the overall drag on Wolverine is lower than on Odyssey because of the smaller drag area.

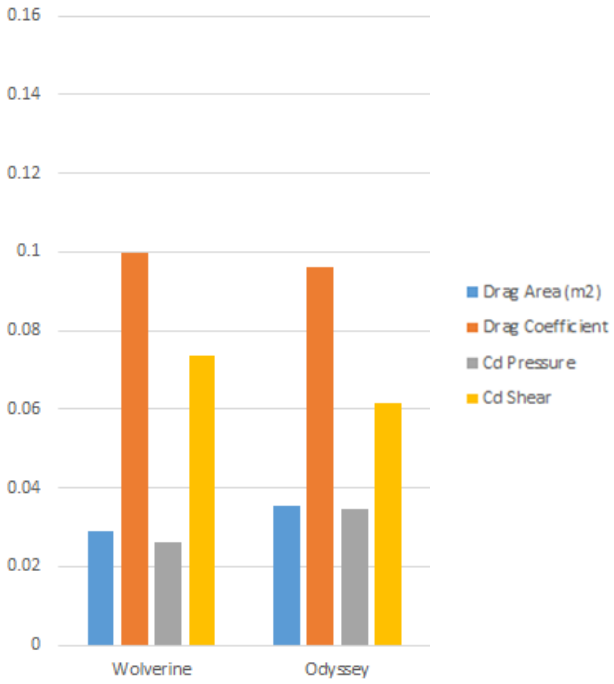

Figure 1.1
Drag parameters of the two hulls as calculated with CFD analysis

Additional CFD shows the streamlines over the hull. As shown in Figure 1.2, the streamlines around Wolverine have significantly fewer vortices than Odyssey. That indicates the flow likely

remains attached throughout the length of the sub. That accounts for the higher skin drag on Wolverine. The vortices on Odyssey are right where the control surfaces are, resulting in a turbulent flow that cannot be used effectively to steer the submarine, which accounts for the issues seen in the last eISR where Odyssey could not be turned.

Figure 1.2

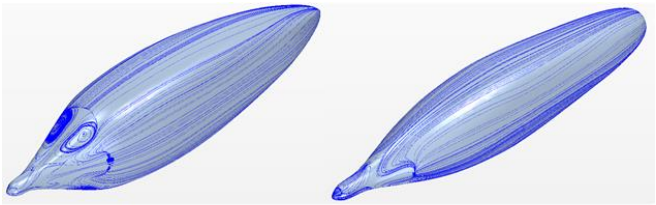

In addition to the lower drag and fewer vortices, Wolverine has an 11% smaller volume. This amounts to a mass reduction of 61 kg and therefore a faster acceleration. These factors were all considered in choosing a hull form we should use for the 13th ISR. Due to time constraints and budgetary issues, we reused a hull form that we had verified would be stable, has low drag, and has low volume.

Despite keeping the same hull, there was a lot of work to be done. We sealed the previous hatch and cut a new pilot hatch. The new hatch is smaller to reduce drag and centered to make the drag forces symmetric across the hull. We also cut a new access hatch that is over the pilot's feet which releases the safety buoy. This hatch serves a dual purpose of safety, which will be better detailed in the safety buoy system, and access, to better remove and install mechanical systems. In addition, it is significantly smaller than the previous access hatch.

Safety Systems:

Air Tank

The pilot has two air tanks. Their primary air is a 30 ft^3 "pony" tank; their backup is a 3 ft^3 bottle for emergencies only. The pony tank is strapped into the submarine and attached to a first and second stage regulator and an air gauge. To ensure the pilot will have enough air with the smaller pony tank we measured several pilots' air consumption both at stationary (such as waiting for the run to begin) and pedaling consumption rates. Both tests were conducted at a depth of 10ft, the max depth of our testing area. The air consumption rate was measured by timing the use of 250 psi for each pilot and calculating surface consumption rate (SCR) using the following formula:

$$SCR = \frac{\left(1-\frac{P_2}{P_1}\right)\frac{V}{A}}{T} \qquad \text{Eq. 2.1}$$

P_2 is final pressure, P_1 is initial pressure, V is the volume of the tank at its maximum capacity, A is the pressure at depth in atmospheres, and T is time elapsed. The results are displayed in Table 2.2 below, with additional data given in Table 2.1.

P_2	P_1	V_f	A
2250 psi	2000 psi	30 ft^3	1.31 atm

Table 2.1

Pilot	Stationary Time (s)	SCR (ft^3/s)	In Motion Time (s)	SCR (ft^3/s)
Female Pilot	517	.0049	151	.0169
Male Pilot	315	.0081	135	.0188

Table 2.2

From this data, we concluded that our pilots have a safe amount of air in the pilot tank at all times. The pilot tank holds 30 ft^3; dividing the largest SCR by the tank capacity gives a time of 26.6 minutes breathing off the tank while pedaling. This provides plenty of air for pre-race and completing a race.

The emergency bottle is attached to the pilot themselves and is intended only for emergencies. It contains enough air for the pilot to safely egress and ascend in case of an emergency. All of our pilots practice an escape and ascent on this bottle in training to ensure they are able to do so calmly and safely in case of an emergency situation.

Access Hatches

There are two hatches in the submarine: one for pilot entry and one to allow for mechanical access, the safety buoy's ascent, and access to the pilot's feet in the event they cannot unclip themselves from the bike pedals.

The pilot hatch is centered on the top of the submarine to allow for symmetric drag forces. The latch mechanism for the main hatch is able to be opened easily both from inside and outside of the hull. It is simply a U-shaped bracket fixed to the hatch and a square peg on the hull, which slides open or closed. The inside and outside of the mechanism can be seen in Figure 3.1. The pilot can open the latch in one of two ways, either by reaching behind their back and manually opening the latch, or by pulling on a cable fixed near the joystick. The cable is connected to an orange ring for ease of grip. The other end connects directly to the latch, which slides open when the cable is pulled. From the outside, the hatch can be opened by sliding the latch mechanism on top. A large red rescue arrow indicates the location of the latch and the correct direction to pull.

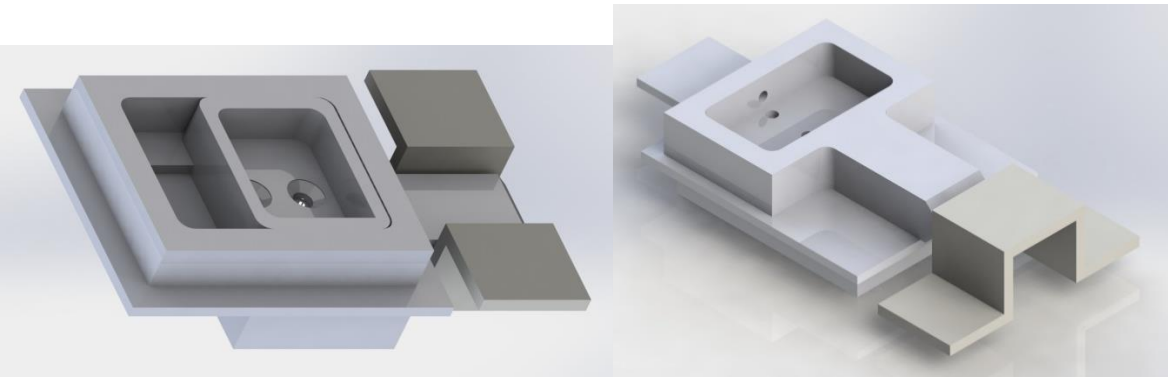

Figure 3.1: Outside (left) and Inside (right) of hatch mechanism

If any component were to fail, the latch would open. The latch is made of half-inch thick aluminum, which will not fail due to shear stresses. The largest potential point of failure in the latch system was the U-shaped bracket's mount separating from the hatch, as it is attached with fiberglass. If it were to fail, the hatch would come off, allowing the pilot to exit but disqualifying us from that run. In order to test that it wouldn't fail, a test specimen was made, identical to the actual mechanism. We calculated the force on the latch using the method below. The pressure difference on the hatch due to water flowing over the top can be calculated with Bernoulli's equation.

$$P = {}^{1}/_{2}\,\rho v^{2} \qquad \text{Eq. 3.1}$$

We assumed a speed of 7 knots, or 3.6m/s. That equates to a pressure of 6.5kPa on the outside if it was at stagnation pressure. Treating water as an ideal fluid, the pressure should be approximately 40% of stagnation pressure. Over an area of approximately 0.39m^2 that amounts to a force of 1kN or 228lb that must be held by the mechanism. It is held by two points, so distributing that weight evenly our mechanism must hold 114 lbs. With a safety factor of 1.5 it should be able to hold 170 lbs. Using a pulley, we applied 200 lbs. to the mechanism, and it held with no failure observed. Due to this test, we are confident that the latch will not fail and will hold the hatch while allowing easy and reliable pilot egress from inside and outside the sub.

The secondary hatch is centered over the pilot's feet to allow access to their feet in the event of an emergency. The pilot's feet are in bike shoes that are clipped to the pedals. They are easy to remove by simply rotating the ankles, but the pilot's feet can also be easily removed from the shoes by removing a Velcro strap. Both the edge of the shoes and the Velcro strap is painted orange so they can be easily seen. The latch mechanism for this hatch is explained below, in the Surface Alert Buoy section.

Surface Alert Buoy:

To allow the surface crew to be alerted to issues with the pilot, we have a buoy that floats to the surface at the release of a switch. The system is weighted so that it will also release if the pilot

stops squeezing the switch. The release of the handle allows the rear hatch to open, which releases the buoy. This also allows for access to the pilot's feet, so in the event of an emergency it is easy to remove them from the bike shoes if needed.

The pilot's interface with the safety system consists of a simple lever handle. This allows the pilot to have a large mechanical advantage, therefore decreasing the force they must use to keep the buoy from deploying. The force applied by the pilot is transferred to the latch with a sheathed cable. The cable used is capable of holding 70lb of force, which is more than could be applied, as will be detailed later.

The latch mechanism in the rear of the sub holds the rear access hatch closed so long as the pilot's handle is compressed. When the hatch is released, the buoy is angled so it will float to the surface, as long as the sub is at any roll angle other than exactly 180 degrees. In that event once the sub rights itself a little bit (which it naturally wants to do because it has a higher center of buoyancy then mass) the buoy will be released. The hatch is attached with a cable so it will open but not float away.

The mechanism itself consists of a spring and two concentric shafts, as seen in the cutaway in Figure 4.1. The spring compresses ½" from fully open to fully closed. That equates to a force of 24lb. The mechanical advantage on the spring and handle decreases that force so it is comfortable for the pilot to hold.

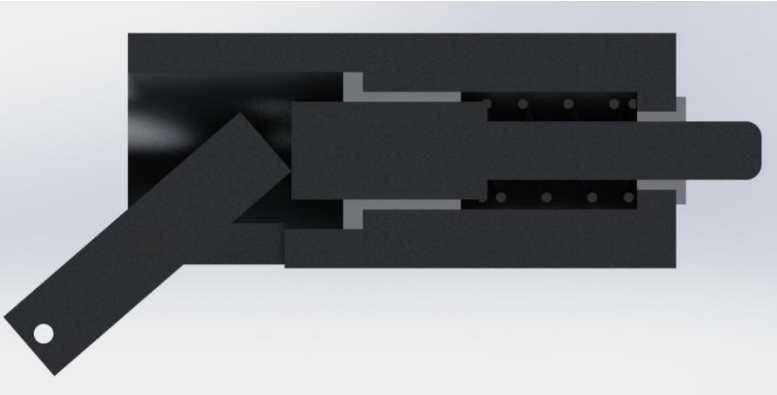

Figure 4.1: Latch mechanism for buoy

The pressure difference on the hatch due to water flowing over the top can be calculated with Bernoulli's equation as shown in the previous section. The same pressure of 6.5kPa applies, but it is over an area of approximately $0.0774m^2$ that amounts to a force of 192N or 43lb that must be held by the mechanism. That force is held by two points, so that value was divided in two, but a safety factor of 1.5 was applied giving us a force it must hold of 32lbs. That is much less than what would cause shear on a ½ in aluminum rod or that would cause the fiberglass to separate, as we showed it could hold over 200lb earlier. In the unlikely event either the aluminum or fiberglass would fail the hatch would open.

Power Transmission

Drivetrain Overview

The drivetrain converts the input of the pilot pedaling to a higher RPM set of contra-rotating shafts via multiple gear sets (Fig. 5.1). The pilot input was taken to be 0.35 HP at 55 rpm. The drive train has 3 gear sets; speed multiplier, bevel gear set, and differential. The speed multiplier is comprised of the input shaft, large spur gear, small spur gear, and transfer shaft. The speed multiplier has a gear ratio of 1:1.6. The bevel gear set is comprised of the transfer shaft, bevel gear, pinion gear, and output shaft. The bevel gear set has a 1:2.5 gear ratio. Spiral bevel gears are used instead of straight cut bevel gears, as the spiral cut allows for constant contact resulting in less noise, fewer losses, and slower gear wear. Together the speed multiplier and bevel gear set have a gear ratio of 1:4; which is capable of gearing up the pilot input from 55 rpm to 220 rpm. The differential is comprised of three small gears, two large gears, output shaft, inner shaft, outer shaft, and two support shafts. The differential serves to divide the torque from the output shaft to the inner and outer shafts. The output shaft is directly connected to the inner shaft and first small gear. There are five gears, with three meshing interfaces, and none of them act to change the gear ratio, therefore the result is an output at the same rpm but with the opposite direction of rotation. The final gear of the five gears connects to the outer shaft (Fig. 5.2).

The gearbox is a two part shell. The two half shells are secured together by nine fasteners. The shell provides bearing pockets where possible. Bulkheads have been added to allow for mounting bearings and bushings where the shell could not. The bulkheads are mounted to the shell with dowel pins. The tolerance of the dowel pin holes allows the bulkheads to be lifted out to access the shafts and other components within the gearbox. The only watertight part of the gearbox is the area that houses the motor that actuates the controllable pitch propellers' motor, while the rest is allowed to flood. It was considered risky to try to create a dry gearbox as that would require many seals that could fail, all of which would increase the friction within the drive train. All components within the flooded portion of the gearbox are made from corrosion-resistant materials or plated with hard chrome. The gearbox has holes to allow the water to drain.

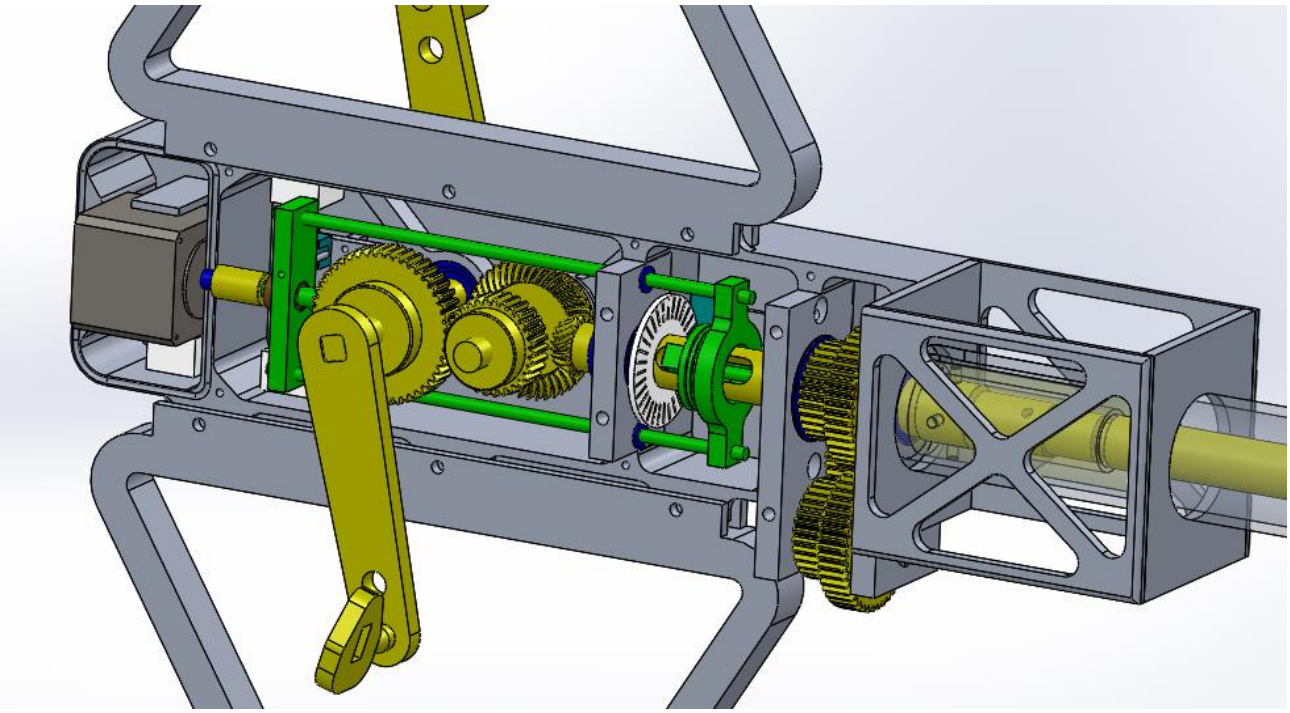

Figure 5.1: Yellow components are torque transferring. Blue components are bearings and bushings. Green components are involved in CPP actuation.

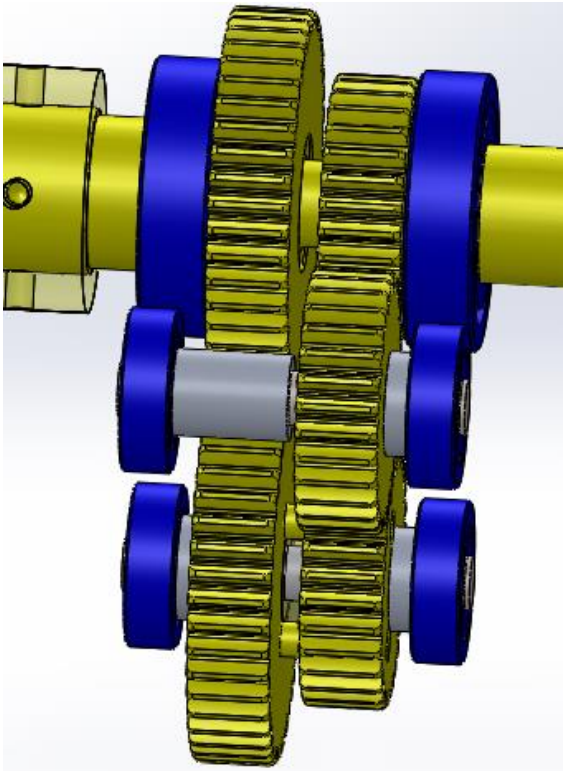

Figure 5.2: The input shaft is shown on the right, and the outer shaft is shown on the left. There is no rpm change as each gear meshes with a gear having the same number of teeth. The large and small gears at the bottom are pinned together.

Material Selection

The materials for the shafts were chosen for corrosion resistance, strength, and machinability. There is a trade-off between strength and machinability; as such the materials were chosen first to satisfy the strength requirements then to allow for better machinability. The second moment of area was calculated by Eq. 6.1, the maximum shear stress within each shaft was calculated by Eq. 6.2, the Von Mises stress was calculated by Eq. 6.3, the safety factor was calculated by Eq. 6.4. The findings from these equations are found in Table 6.1.

$$J = \frac{\pi(r_o - r_i)}{64} \qquad \text{Eq. 6.1}$$

Where J is the second moment of area, r_o is the outer diameter, and r_i is the inner diameter of the shaft.

$$\tau = \frac{Tr_o}{J} \qquad \text{Eq. 6.2}$$

Where τ is the shear stress, T is torque, r_o is the outer diameter, and J is the second moment of area.

$$\underline{\sigma_H} = \sqrt{\frac{1}{2}[(\sigma_1 - \sigma_2)^2 + (\sigma_2 - \sigma_3)^2 + (\sigma_3 - \sigma_1)^2]} \qquad \text{Eq. 6.3}$$

Where σ_H is the Von Mises stress, $\sigma_1$is the first principal stress, $\sigma_2$is the second principal stress, and $\sigma_3$is the third principal stress. When torque is the only major force acting on the shaft, the following assumptions can be made; first principal stress is the shear stress, second principal stress is the negative of the shear stress, and the third principal stress is zero.

Table 6.1: Shaft selection results

	RPM	in*lb	HP	OD	ID	J	shear stress	Von Mises Stress	Material	Yield strength	Safety Factor
Input Shaft	55	401	0.35	0.625	NA	0.0075	16739	28992	17-4 SS	145000	5.0
Speed Multiplier Shaft	88	251	0.35	0.591	NA	0.0060	12392	21462	17-4 SS	145000	6.8

Pinion Shaft	220	100	0.35	0.5	NA	0.0031	8153	14121	17-4 SS	145000	10.3
Inner Shaft	220	50	0.175	0.625	0.385	0.0064	2438	4223	304 SS	31200	7.4
Outer Shaft	220	50	0.175	1	0.75	0.0335	745	1291	6061-T6 Al	40000	31.0

All gears are appropriately constrained by spacers on the shafts. Torque is transferred between shafts and gears through keys. To prevent the keys from moving out of position, they are all secured with set screws. All bearings are shielded to prevent debris from entering the races, and full stainless steel construction to prevent corrosion. When a spiral bevel gear set is loaded with a torque, the small pinion gear will either be sucked into the bevel gear or pushed away from the bevel gear, depending on the direction of rotation. This is caused by the spiral engagement of the teeth. To prevent the pinion from disengaging from the bevel gear, the pinion is backed with a thrust bearing and rotated such that the pinion gear is forced away from the bevel gear but is prevented from moving due to the thrust bearing (Fig. 6.3).

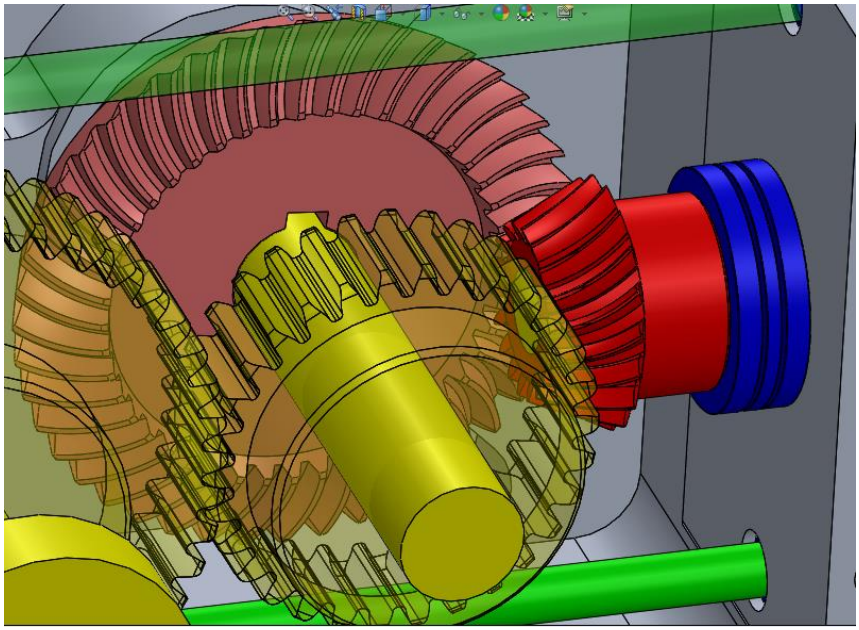

Figure 6.3: The pinion gear (red) pushes against the thrust bearing (blue) which is restrained by the bulkhead. This allows for smooth operation of the bevel gears with minimal losses.

The outer shaft connects to the front propeller hub, and the inner shaft connects to the back propeller hub. Torque is transferred from these shafts to the hubs. The hubs are too long to key, therefore the torque must be transferred by another means. The end of the outer shaft is squared off and is received by the front hub with a square hole. A screw then restrains the hub from being separated from the shaft. The wall of the inner shaft is too thin to be squared off, therefore a set

of two fasteners transfer torque to the back hub and prevent the hub from separating from the shaft. As both of the areas will be stress concentrations, finite element analysis, FEA, was performed on the ends of these two shaft. The results of the FEA on the inner shaft are presented in Figures 6.4 and 6.5. The results of the FEA on the outer shaft are presented in Figures 6.6 and 6.7.

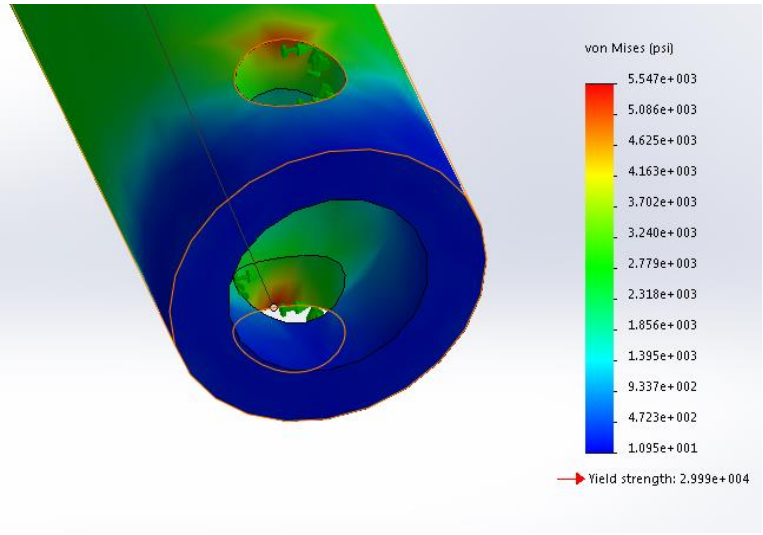

Figure 6.4: FEA of the inner shaft shows a maximum stress of 5,547psi which is well below the yield strength.

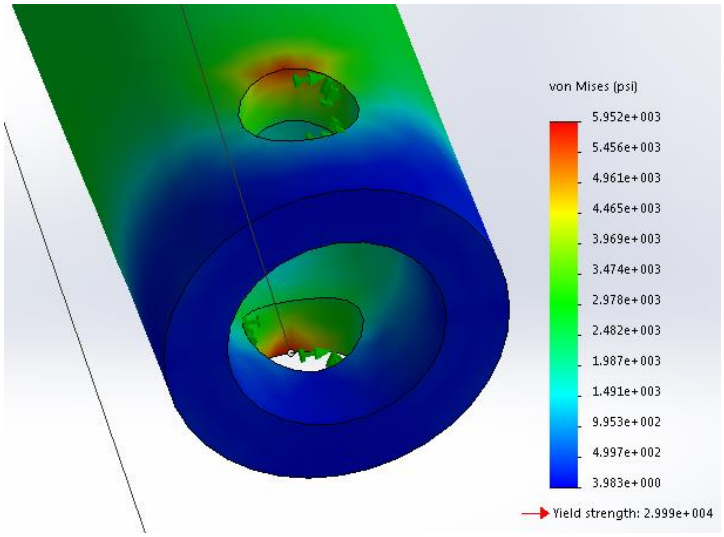

Figure 6.5: FEA results of the inner shaft with a mesh density twice that of the FEA from Figure 6.4. The results of the doubled mesh are within 7% of the original FEA results. This shows that the FEA results are independent of mesh density given the large amount of uncertainty associated with FEA. The stress in areas of the shaft not influenced by stress concentrations, 4000 psi, is close to the calculated Von Mises stress of 4200 psi.

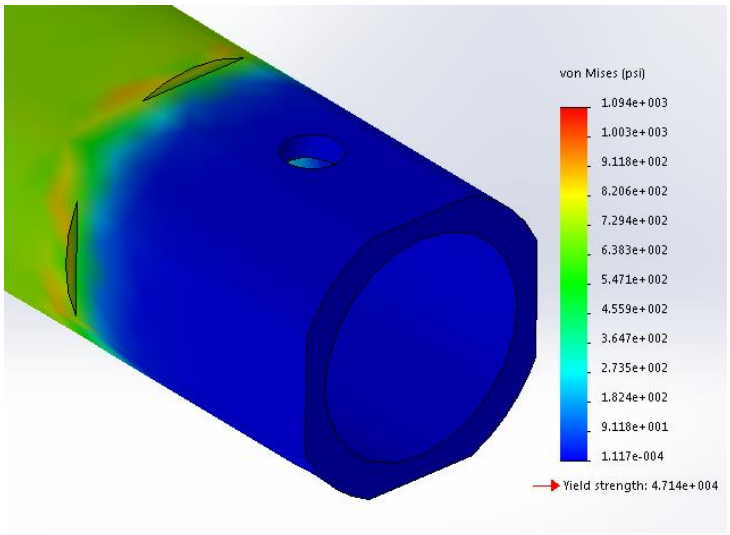

Figure 6.6: FEA of the inner shaft shows a maximum stress of 1,094psi which is well below the yield strength.

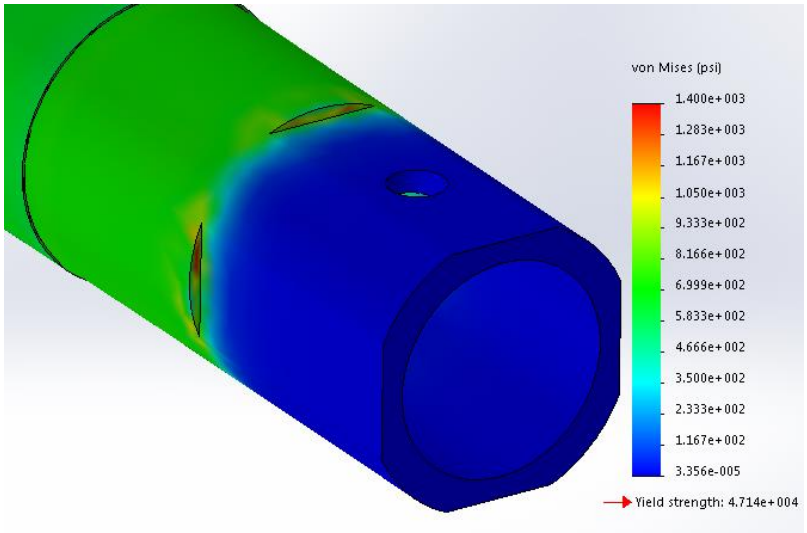

Figure 6.7: FEA results of the inner shaft with a mesh density twice that of the FEA from Figure 6.5. The results of the doubled mesh are within 21% of the original FEA results. This is too much to claim mesh independence.

Findings from the FEA on the end of the inner and outer shafts can be summed up as follows. The average stress in the inner shaft where there are no stress concentrations is within 5% of that calculated by Von Mises stress criterion. Mesh independence was proven for the inner shaft. The combination of these two results gives weight to the validity of the FEA results of the inner shaft, which suggests that the shaft will not yield. The average stress in the outer shaft where there are no stress concentrations is less than 35% of the calculated Von Mises stress. Mesh independence could not be proven for the outer shaft. The combination of these two results denies validity to the FEA results of the outer shaft, leaving the results to be inconclusive. As always the results of

FEA must be taken cautiously even if mesh independence is proven with great success. Given the large safety factor associated with both of these results and that of the Von Mises stress calculation, we are confident that the shafts will not yield under the standard operating conditions of 0.35HP input at 55rpm.

Mounting

The drivetrain and controllable pitch mechanism must be easily removable. The CPP/DT can be tested with few additional components, as the CPP and DT are rigidly attached together by the tube that spans between them. This structural tube connects the hub assembly to the gearbox (Fig. 7.1). To allow for easy removal there are four screws that hold the DT support to the hull brackets and no screws at the hubs (Fig. 7.2). The cowling that supports the hubs is large enough that the hubs can pass through after the propellers are removed. (Fig. 7.3).

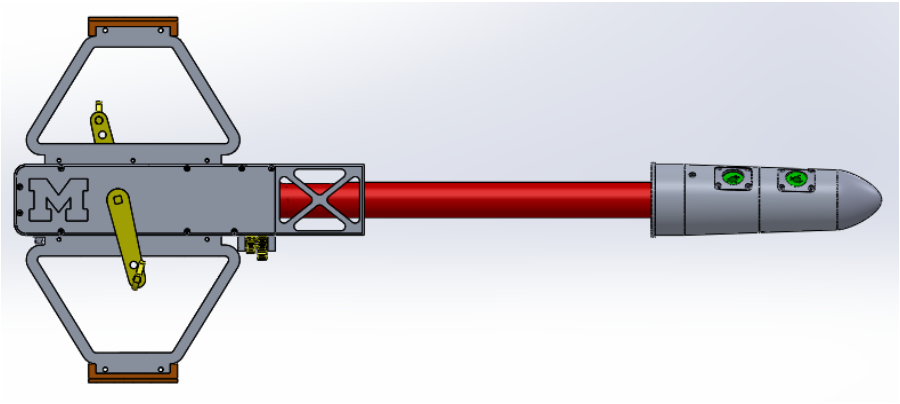

Figure 7.1: The structural tube (red) rigidly connects the hub assembly and gearbox.

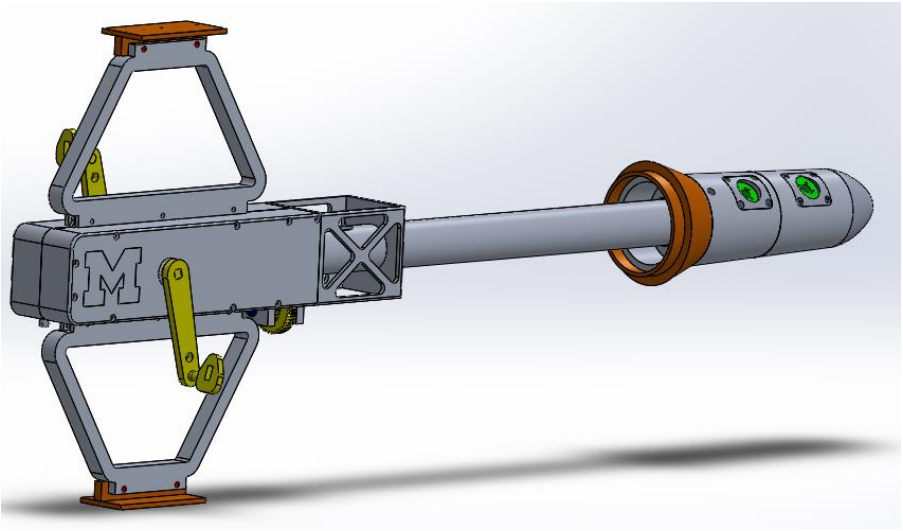

Figure 7.2: The components in orange are permanently attached to the hull. The placement of the four mounting screws is noted by the four red holes.

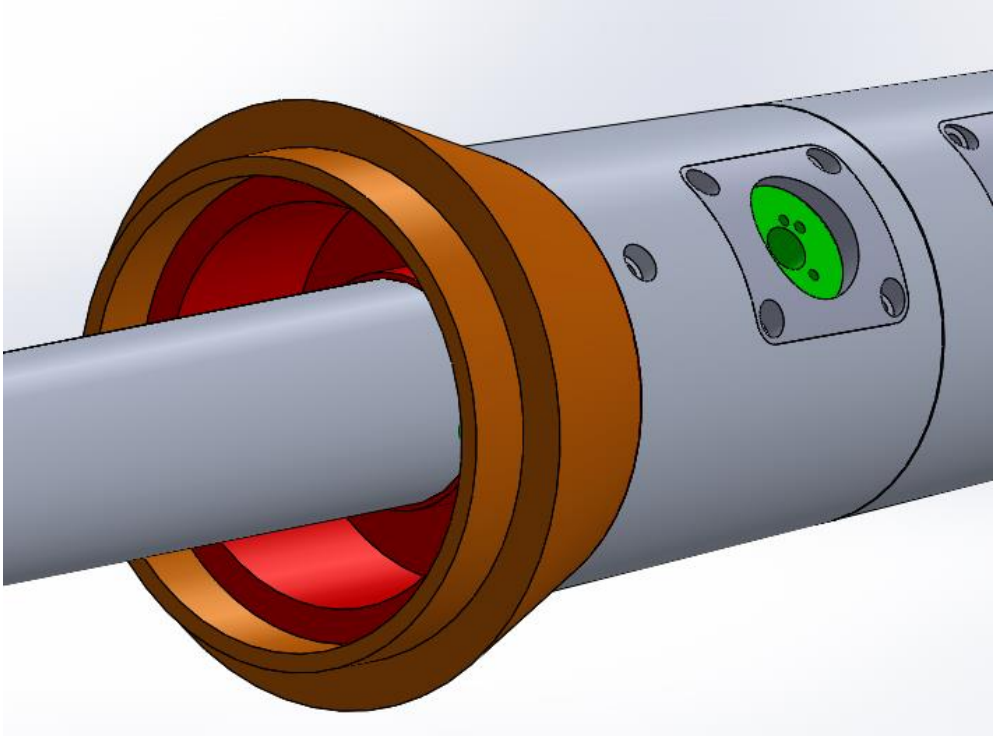

Figure 7.3: The Cowling (orange) is permanently attached to the hull. The hub support (red) rests with the cowling. The hubs can pass through cowling when the propeller blades are not attached.

Propellers

Controllable Pitch Mechanism

The CPP is has two assemblies; the hub assembly (Fig. 8.1) and the control assembly (Fig. 8.2).

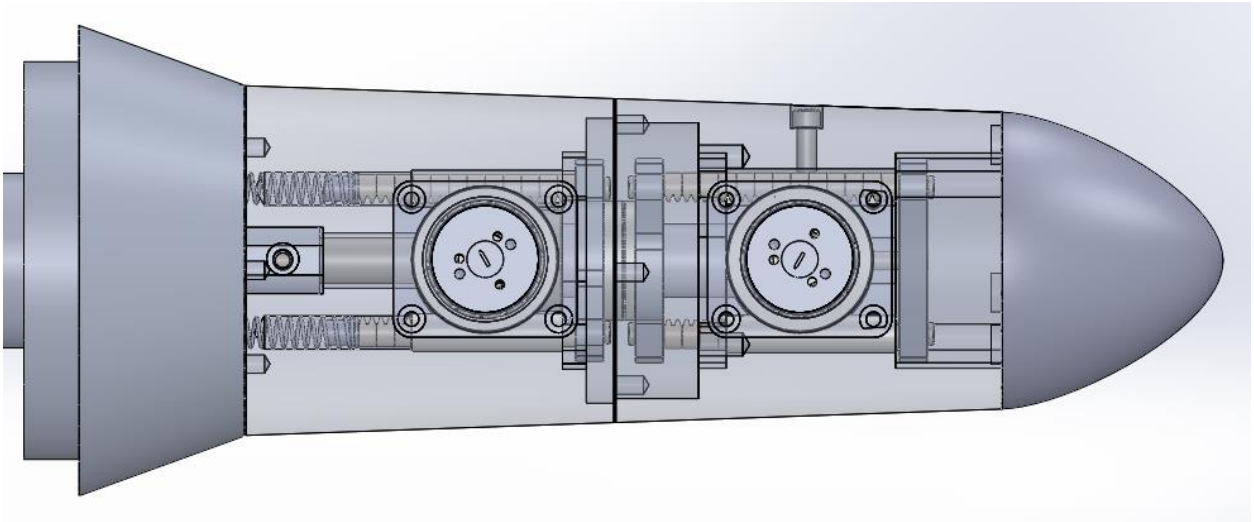

Figure 8.1: The hub assembly is located at the back of the submarine. The propeller blades attached to this assembly.

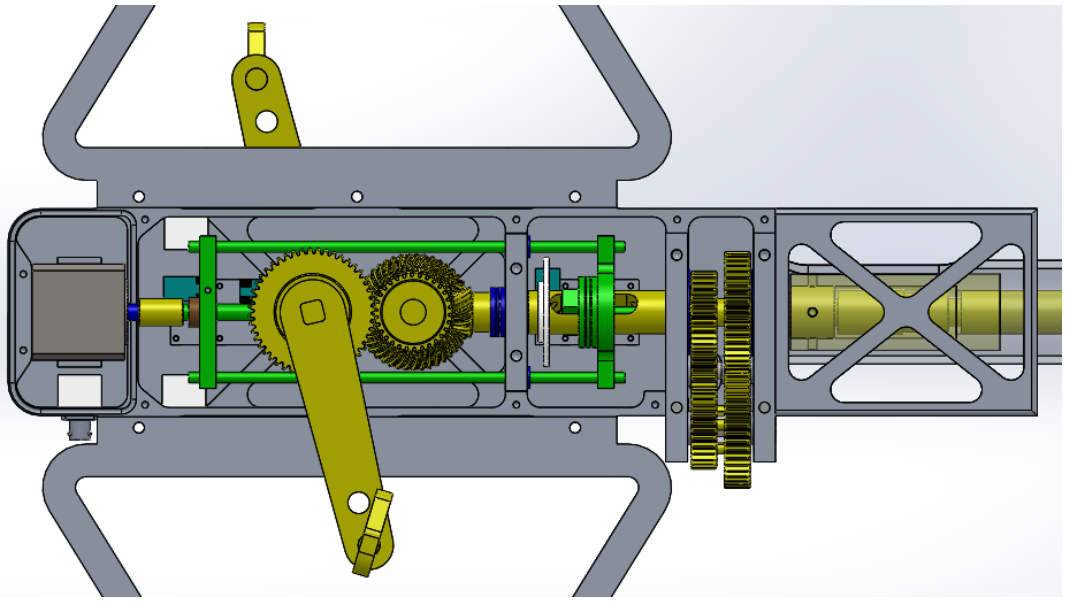

Figure 8.2: The control assembly is comprised of the green and teal components, associated bushings and bearings, motor (dark grey), and the shaft connector (yellow) that transfers torque from the motor to the lead screw.

The CPP system is designed to modulate the pitch of the propellers. To meet this requirement, each propeller is mounted on a prop connector, which is mounted to a gear. There are bearings at the top and bottom of the prop connector to allow for smooth rotation of the propeller even when thrust is causing a moment on the shaft (Fig 8.3).

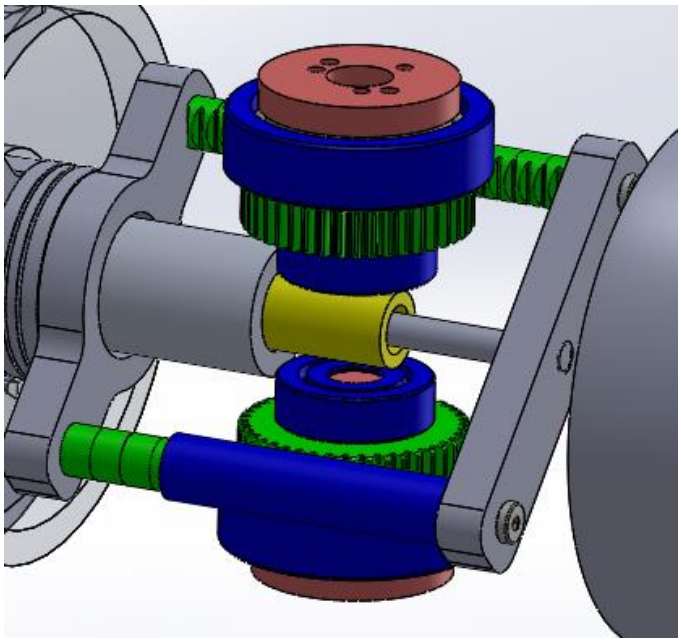

Figure 8.3: The prop connector (pink), is supported by two bearings (blue), which sandwich the pinion gear (green), and is caused to rotate by the rack (green).

The prop connector is pinned to the pinion gear so that they rotate together. When the rack translates, it causes the prop connector to rotate via the pinion gear. Each hub has a rack and pinion set for each propeller blade, and they all move together. The preload springs keep the actuation system in compression. It is important to keep the actuation system in compression, as the lack of compression would allow the prop connector to rotate freely. The preload springs push against the racks in the front hub (Fig. 8.4). This force is then transmitted through a set of connectors and a thrust bearing onto the set of racks in the second hub. This force is finally opposed by the final connector that bridges the second set of racks and connects to the actuator rod (Fig. 8.5). It is important that there is a thrust bearing between the two sets of racks as they are rotating in opposite directions. An appropriately sized cavity accommodates the rotating parts that pass between the hubs.

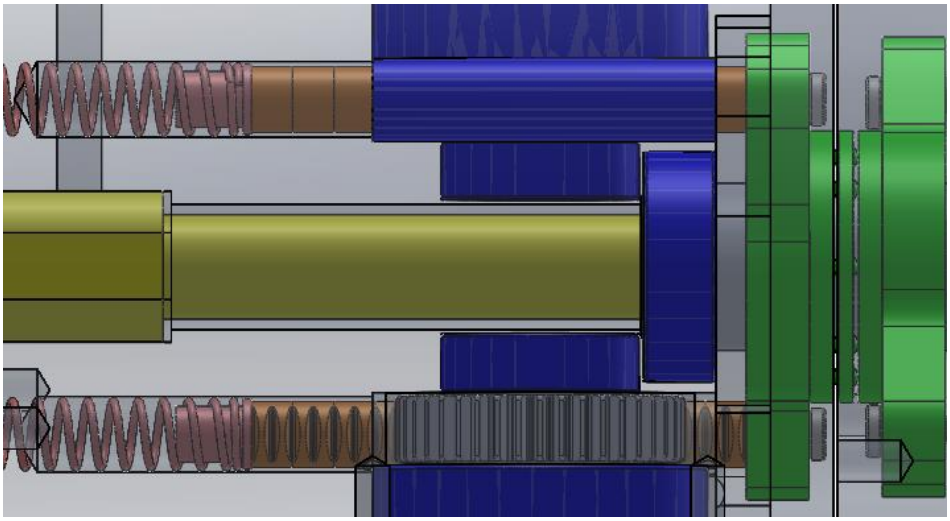

Figure 8.4: The preload springs (pink), push against the first set of racks (orange), which then push against the connectors and thrust bearing (green).

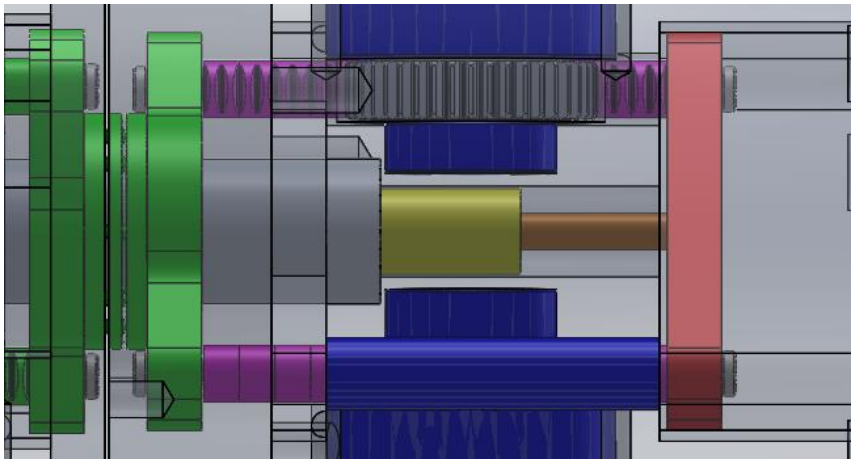

Figure 8.5: Force is transmitted from the connector and thrust bearing (green), to the second set of racks (purple), to the final connector (red), then to the actuator rod (orange).

As the actuator rod is pulled forward by the CPP control mechanism, the pitch of the propellers is increased and the force of the springs increase. The force applied by the springs varies from 12-24 lbs, depending on how much the springs are compressed. The highest spring force is associated with the highest propeller pitch, and the highest torque applied by the propeller blades by the thrust being generated. The position of the center of pressure of the propeller relative to the axis of prop connector determines how much torque the blade applies to the actuation system.

The actuator rod must rotate with the back hub and be able to translate back and forth while concentric within the inner shaft. To accomplish this there is a section of the output shaft that is notched for a small transfer block. This transfer block is caused to rotate by the notched shaft it is within, is pushed forward by a thrust bearing (Fig. 8.6), and is pulled backward by the compression caused by the spring preload in the hubs. This thrust washer is pulled forward by the connection it has to the acme lead screw (Fig. 8.7). As the acme lead screw is rotated by the stepper motor, the nut on the acme lead screw translates causing the actuation of the CPP.

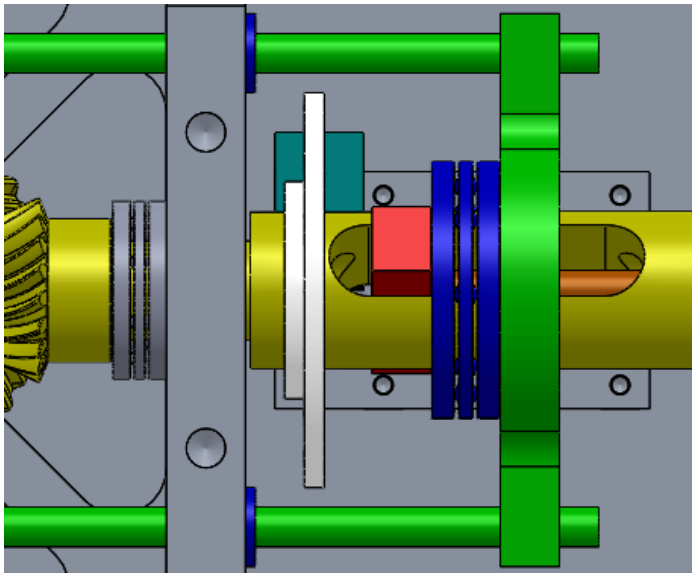

Figure 8.6: The transfer block (red) is pulled back by the actuator rod, and pushed forward by the thrust bearing (blue). The thrust bearing is pushed forward by the connection (green) to the acme lead screw.

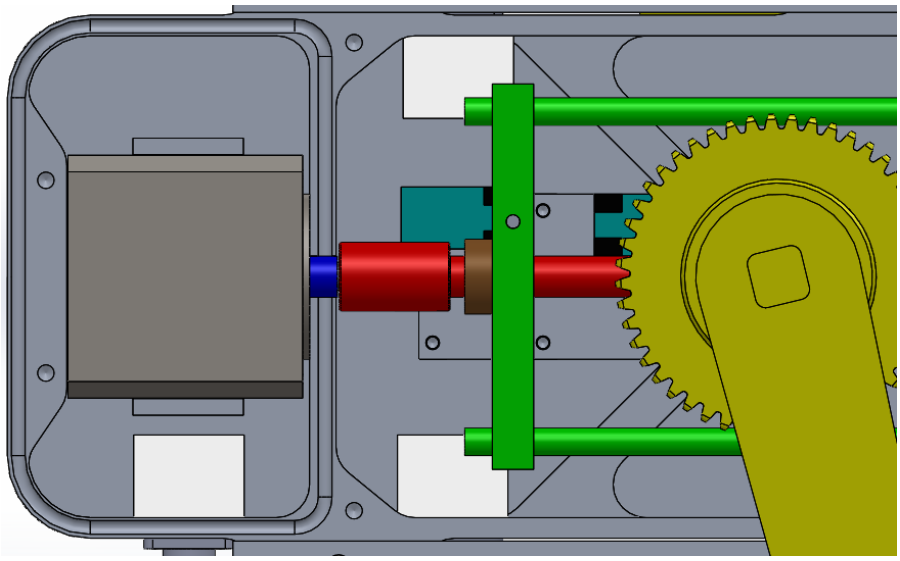

Figure 8.7: As the stepper motor (dark grey) rotates the acme lead screw (red), the acme nut (brown) translates along the acme lead screw, and with it the connectors (green) move.

Control System

The control system is comprised of the stepper motor, limit switches, speed sensor, microcontroller, and the motor driver. The CPP uses a closed loop proportional control system. The control system can be described by a block diagram of a controller/actuator, thrust generated, in water disturbance, the submarine, a feedback loop, a microcontroller, and various gains (Fig. 9.1). Thrust is a function of the pilot input rpm and the pitch of the propeller. The pilot input has been assumed to be a constant 55 rpm to simplify the diagram.

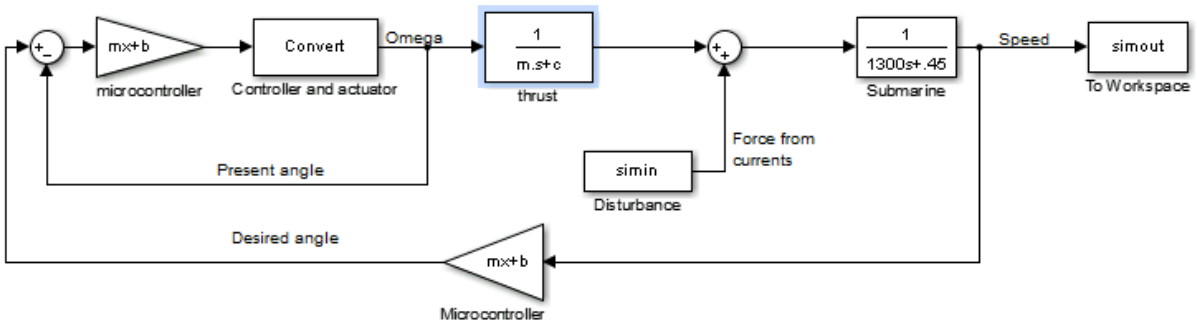

Figure 9.1: Block diagram of the control system

Given that the stepper motor being used is far more powerful than the force opposing it, the assumption that there is no error between the controller and actuator is safe to make. The implication of this is that when the controller tells the stepper motor to step it does so without missing a step. This allows us to create a closed loop feedback system by using the speed measurement to compute the optimal propeller pitch angle, the set point, then comparing this to

the present angle to get the error. The error is then used by the proportional control program to determine how many steps the motor driver should send to the stepper motor driver to eliminate the error. The speed measurement is taken from an anemometer adapted to be waterproof and recalibrated for the properties of water. Alternatively the control system can be used in conjunction with the rpm sensor to keep the pilot pedaling at a constant rpm by varying the load on the drivetrain by adjusting the propeller pitch (Fig. 9.2). This however does not ensure the optimal pitch is being achieved.

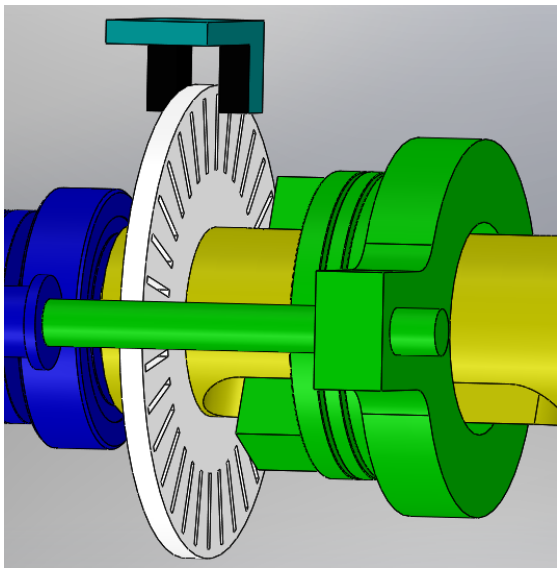

Figure 9.2: The rpm sensor is an underwater optical interrupter with an encoder disk that has 32 slots which corresponds to 32 pulses per revolution of the output shaft.

When the control system is first powered up it will travel the flag on the acme nut plate to the two optical interrupter limit switches to establish the home position and travel limit of the actuator (Fig. 9.3). The limit switches prevent the CPP from being actuated outside of the safe operation area. This a soft limit as limiting is done by electronic hardware not a physical limit. When the flag reaches a limit switch, the control program will not actuate the CPP any further in that direction. The actuator starts at a low pitch not zero pitch. The time spent under 2 knots is such a short duration that it is ok to start the propeller pitched for 2 knots. It should also be noted that at zero speed the optimal pitch would be zero, which would produce no thrust.

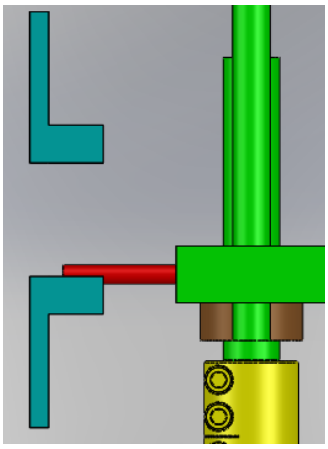

Figure 9.3: The flag (red) is a dowel pin attached to the acme nut plate. The flag is positioned to break the beam of the optical interrupter before physical damage would occur to the system.

The electronic connections to the gearbox are made by IP69K connectors. Each connector passes through the wall of the gearbox where it is fastened to a sealed and dry backshell. Within the backshell, the wires from the motor or sensor are soldered to the connector. The backshells are potted to prevent any moisture from damaging the electrical connection.

Propeller Design

The propellers were designed using a fortran lifting line program written by Art Reed, a friend of the team and engineer at NAVSEA. The propellers are wake adapted and designed to be contra rotating. The wake was estimated using Solidworks' flow simulation software. That was then put into the lifting line program. That code outputs the lifting line of the propeller from which a model of the propellers was designed and manufactured. Due to limitations in team experience with propeller manufacturing and time the team did not machine the propellers ourselves, but instead had an outside company machine them. Hopefully in the future this is something we are able to do ourselves.

Non-Propeller System

In addition to our primary propeller driven system we designed a highly experimental non-propeller system. Due to the experimental nature we opted to not enter wolverine in both the propeller and non-propeller divisions, but we do plan on trying the system at the race. The propeller and non-prop systems can be exchanged in less than 20 minutes and have the same mass and center of mass underwater so they do not effect buoyancy.

The system works using an impeller to highly pressurize the incoming water and a duct to direct that pressurized water out and provide propulsion.

In addition to our primary propeller system we designed an experimental non-prop system for this year. We are not registered in the non-propeller category so will be using the system purely for experimental purposes and data testing for the future. The system relies on a duct and an impeller to propel the submarine. It is internchangable with our standard propeller drive in less then 20 minutes and has the same center of gravity and weight underwater. The system is comprised of four major components; the ducting, the gearbox, the mounting mechanism, and the impeller itself.

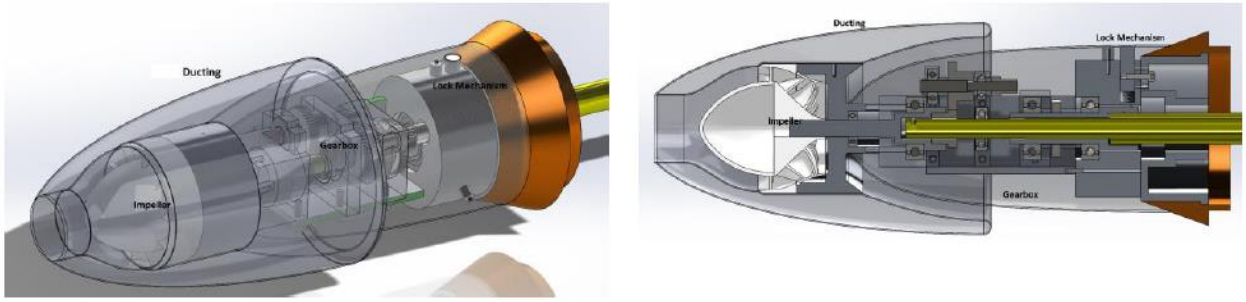

Figure XXX: Impeller system CAD and Cutaway view

The ducting is made of fiberglass from a tooling board mold. The ducting controls the flow of water into the impeller and directs the exiting water.

The gearbox converts the 220 RPM that is normally provided to the propellors into 2700 RPM that is required by the impeller. This is done with three sets of gears. The gearbox is enclosed in another fiberglass casing that helps direct the water into the ducting.

The impeller takes the rotation of the shaft and transforms the water from an axial flow to a very fast radial flow. Six different impeller designs were created and three of the most promising designs were 3D printed and a test mechanism to be constructed to measure the amount of thrust that each impeller could produce. With the impeller and nozzle underwater, a DC motor was supplied with 350watts of power, and the thrust as measured by the spring scale was recorded during the tests. The highest thrust was recorded at 4lbf and that design was used for the rest of the impeller system.

The system is mounted with a quick lock system to ensure it can be easily tested without interfering with our other systems. The mechanism works by pushing a spring loaded button on the back plate of the gearbox which pushes a screw down with it. The entire module can then be lined up with the existing mounting face on the submarine and the screw would fit in the slot. When the button is released, the screw slides up the slot, similar to a chain lock on a door, locking this entire module in place. In order to help support the load of the entire impeller module, four dowel pins were placed between the module and the mounting face on the submarine.

Electronics

This year's electronics system is the second of a four year succession of goals toward near-complete automation. The eventual goal for the 2017 ISR is to require the pilot to only pedal.

Last year for the EISR we tried electronics for the first time. The electronics were used to control the pitch of our propellers, but we encountered a lot of issues with waterproofing and sensing speed. This year we continued attempting to adjust pitch, plus data logging various control-related parameters and improving on the LCD display system. The speed of the submarine and propeller RPM were already necessary for the CPP, but they are now being data-logged as well. Additions for this year include an LCD display as well as systems measuring and recording dive plane angle, rudder angle, submarine depth, and submarine pitch. The hope is that the data collected in testing and at the competition can be used to write PID loops next year to smooth out the controls (mechanically) and keep the submarine traveling in a straighter direction to decrease run time.

The electronics for this year have several main compartmentalized sections. Both the main control housing and battery housing are semi-permanently sealed and the stepper motor is in its own sealed box inside the drivetrain. The box containing the data logger is a waterproof Otterbox case. Everything else (angle sensors, depth sensors, end limit switches for the CPP stepper motor, RPM sensor, and speed sensor) are encased in epoxy to prevent water damage. Their cables have also had epoxy vacuum-forced into the insulation to prevent water penetration through the connectors. We separated the components in hope that, in the unlikely case of a seal failure and leak, only a small portion of the electronics will be damaged. Since all of the data is routed to the main control board, resistors have been placed on all connections so that if anything shorts out anywhere in the sub, the damage will be isolated to that component. Fuses are also placed in line with the battery for the same reason.

The main control board is a PJRC Teensy 3.1, ARM-based microcontroller. We had custom-made boards printed for this and the angle sensors. All of the data from the submarine comes directly into the Teensy through the PCB (primary control board). It is then used in two main algorithms. One of the algorithms takes in speed and RPM data and sends commands to stepper motor in order to change the pitch of the propellers. The second algorithm takes in all data and transmits it to the data logger.

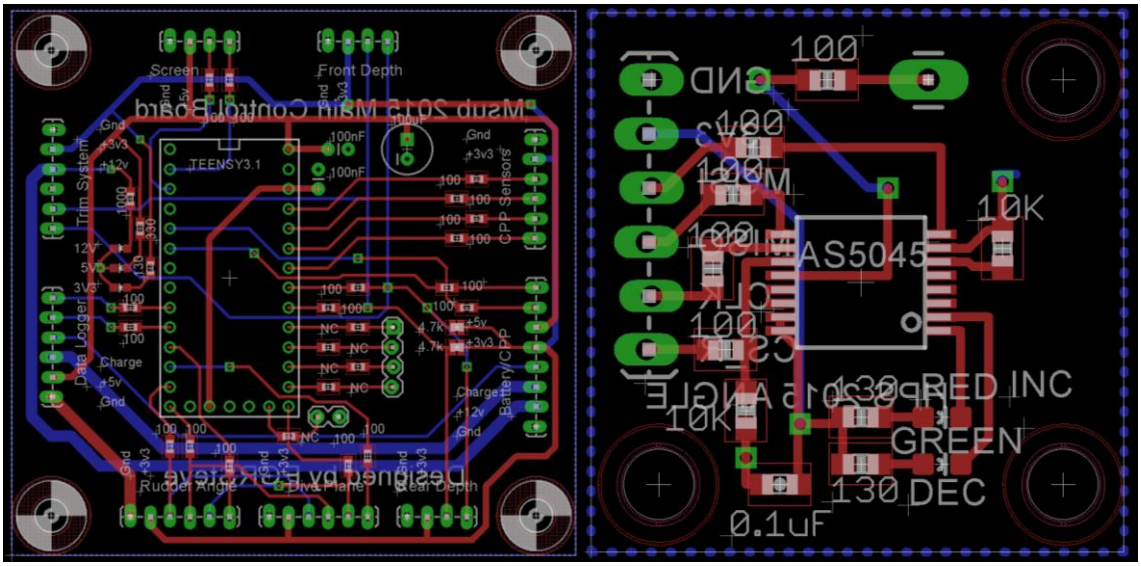

Figure 10.1: Custom made boards. Left is main board, right is angle board

The data logger is an Arduino Pro-Mini microcontroller with an SD card shield containing buttons and switches for references in the data. All of the data comes directly from the Teensy through the Teensy and Arduino's Serial Ports. When a button is pressed, that button's color is recorded in the data. With standard convention, green means start (of the run) and red means stop. Because the data logger is the only non-sealed compartment, it also contains a charging port that goes to the battery compartment so it does not need to be opened.

Each of the angle sensors for the control surfaces is an Austrian Microsystems AS5045 angular Hall Effect sensor. This is mounted to the other of custom printed circuit boards. When a dipole-oriented magnet is held up to the chip, it can detect the angle of the magnet (with the axis of rotating going from perpendicular to the chip out through the center of the magnet). These are ideal because there is no mechanical connection, so the sensors need only be given a short time on startup to zero themselves. The depth sensors are simple pressure sensors running in the I^2C interface of the Teensy. One is mounted in the front and the other in the back. The algorithm that collects the data also averages the two to give mean depth and calculates the pitch angle of the submarine. The speed sensor is a simple anemometer recalibrated for use in water. Each of the stepper limit switches and RPM switches are optical interrupt switches similar to that on garage doors. When the stepper reaches the rear or forward limit of its pitch travel, the beam is broken and the stepper stops moving to avoid damaging either the stepper or the components of the CPP system. The RPM switch is activated by a rotating disk attached to the drive train with slots so the beam is cut and uncut many times per shaft rotation. The amount of interrupts during a given time interval is then used to calculate the RPM.

Last is the LCD screen made by 4D systems. It simply has displays data sent to it from the Teensy in order to aid the pilot in operating the sub. It displays error messages and the same data that is taken in by the teensy.

Controls

The controls of Wolverine were initially designed with the intent to use pneumatic hydraulic pistons to transfer the input of the pilot to the back control surfaces. The change from the use of cables to hydraulic lines was to allow for easier integration of fly by wire controls in the coming year. To allow for hydraulic controls to fit in the confined spaces of the submarine we used pneumatic pistons and filled all of the lines with water as our incompressible fluid.

In our initial small scale tests of the system we found filling the lines with water and evacuating all air out of the lines was an effective way to move the pistons in a one to one motion. As we went to a full scale setup to install within our submarine, we were having trouble filling the lines with water as we had the pistons setup in much longer lines which we could not completely evacuate with air which then did not allow us to have a one-to-one motion between the front and back of the controls. We did however create a backup system based on previous year's cable based designs.

The controls that will be used for competition have followed in the previous iterations of the University of Michigan's controls designs. We remade our double handle joystick as the pilots found the ergonomics of it to be better than the ergonomics of a single handle joystick.

The back set of controls have made the greatest amount of progress over our design iterations. We use a single plate design were all four control surfaces exist on their own shaft. This allowed us to put all of the control surfaces on that one plate making the installation and the inevitable repair easier. The dive planes and rudders act in unison through a series of cable lines traversing the plate this saved weight in the back as we considered the use of gears, however, decided against it to save weight.

The plate is installed through four mounting points which line up in parallel with the four control surfaces. This aligns the dive planes in the submarine. To hold the plate in place the four dive planes, which were manufactured from a mold and casting resin have a slot milled into the male shaft which aligns with the pin female tube to take up the torque created by the control surfaces. To hold the dive planes from falling out, 4 shaft collar slots were added to the exterior part of our dive plane mounts. This allowed for quick removal of the dive planes which was a top priority in our design requirements as we often need to remove the dive planes.

The wire controls have proven themselves successful in the past. This allowed them to be a solid backup in the event that the new hydraulic controls would not function successfully. We are continuing on with the intention to build the fly by wire system for next year at the EISR.